Cite this article
Zawrah MF, Ngida REA, Abo Sawan SE and El-Kheshen AA (2025)
Effect of MnO_2 nanofibres on the properties of geopolymers fabricated from waste clay.
Proceedings of the Institution of Civil Engineers – Construction Materials **178(6)**: 275–285,
https://doi.org/10.1680/jcoma.25.00010

Research Article
Paper 2500010
Received 06/02/2025; Accepted 24/06/2025

Emerald Publishing Limited: All rights reserved

Construction Materials

Effect of MnO_2 nanofibres on the properties of geopolymers fabricated from waste clay

M. F. Zawrah
Refractories, Ceramics and Building Materials Department, National Research Centre, Cairo, Egypt; Pharos University in Alexandra, Alexandria, Egypt (corresponding author: mzawrah@hotmail.com, mahmoud.zawrah@pua.edu.eg)

Rehab E. A. Ngida
Refractories, Ceramics and Building Materials Department, National Research Centre, Cairo, Egypt

S. E. Abo Sawan
Refractories, Ceramics and Building Materials Department, National Research Centre, Cairo, Egypt

A. A. El-Kheshen
Glass Research Departments, National Research Centre, Cairo, Egypt

This study focuses on fabrication of geopolymers reinforced with chemically synthesised MnO_2 nanofibres, as alternatives to traditional cement-based materials. MnO_2 nanofibres were investigated by X-ray diffraction technique, transmission electron microscope, and particle size analyser. Different geopolymer batches were prepared using Feeder's waste-clay and alkali activator after curing at 70°C. These geopolymers were reinforced with 0.1, 0.3, and 0.5 wt.% MnO_2 nanofibres. The mineralogical composition and microstructure of prepared geopolymers were investigated by X-ray diffraction and scanning electron microscope, respectively. The physical properties were determined according to the Archimedes rule, while the compressive strength was measured by the suitable testing machine. The results showed that MnO_2 nanofibres were successfully synthesised by the proposed hydrothermal method. Moreover, the synthesised MnO_2 nanofibres were successfully utilised for reinforcement of geopolymers. The addition of fibres up to 0.3 wt.% has a significant effect on the physical properties, microstructure, and compressive strength of prepared geopolymer, while the addition of 0.1% or 0.5% changed the properties. The geopolymer sample that included 0.3 wt.% MnO_2 fibres exhibited the lowest porosity value (28.47%) and highest compressive strength (28 MPa) among the tested geopolymers. These interesting properties make them applicable for many structural and building applications.

Keywords: feeder's waste clay/geopolymers/mechanical properties/MnO_2 nanofibres/properties/reinforced geopolymer

1. Introduction

Generally, it has been recognised that the polymer is a large molecule composed of small molecules bonded together. Geopolymer is a type of inorganic polymer that comprises of alumino-silicate groups connected together in three-dimensional networks through alkali/alkaline metals. It is a cementitious eco-friendly material that can replace ordinary Portland cement that emits CO_2 during its manufacturing, consequently polluting the environment. Due to its unique form, shape, and composition, geopolymer demonstrates outstanding physical, thermal, and mechanical properties. To reduce CO_2 emissions, lower energy consumption, decrease costs, and create a binding material with excellent characteristics, the advancement of industrial geopolymer should be prioritised (Korniejenko *et al*., 2020a, 2020b). Geopolymerisation occurs via a polycondensation reaction involving alumino-silicate groups, which consist of aluminum and silicon atoms in the network. This process takes place in the presence of a highly concentrated alkali activator, which can be a combination of sodium hydroxide (NaOH) and sodium silicate (Na_2SiO_3), or potassium hydroxide (KOH) and potassium silicate (K_2SiO_3) (Gailitis *et al*., 2020; Łach *et al*., 2019; Reckard *et al*., 2013; Silva *et al*., 2020; Silva and Thaumaturgo, 2003). The sources of alumino-silicates are either natural/artificial materials like meta-kaolin (calcined kaolin at about 850°C), zeolite, minerals, pure aluminum/silicon oxides, or industrial wastes (various by-products), for example red mud (RD), glass waste, mine waste, ashes, and blast furnace slag granulated (BFS), or other slags (Davidovits, 2020; Samal and Blanc, 2021; Zawrah *et al*., 2022a; Zawrah *et al*., 2025). The stages of geopolymer fabrication include grinding of raw materials, preparation of batch composition, mixing with alkali activators, moulding, and finally curing in humidity or air at room temperature or a temperature below 100°C for 24/48 h. The de-moulded geopolymer can be further cured for a longer time in air or humidity before testing. The geopolymers are interesting materials that can be applied in several applications as construction and building materials, restoring materials, fire-resistant materials, catalysts for biodiesel production, as absorbents for removal of pollutants or toxic chemicals from wastewater, waterproof roof-coatings, biological applications, and encapsulation. One of the most important properties needed for geopolymer is the mechanical strength or fracture toughness. There are many techniques that are used for improving the mechanical properties of geopolymer. One of those techniques is the reinforcement of geopolymer by fibres (Ke and Baki, 2021). Fibres in geopolymers serve to limit and reduce crack propagation, thereby increasing toughness, enhancing durability, and suppressing brittle behaviours and deformation, which ultimately improve

Downloaded from http://ftp.nowpublishers.com/jcoma/article-pdf/178/6/275/10176839/jcoma.25.00010en.pdf by guest on 05 August 2026

mechanical properties (Abo Sawan *et al*., 2020; Khale and Chaudhary, 2007). Moreover, the fibre can improve the physical properties of geopolymer and flexural strength of geopolymer composites (Arthiban and Vaithianathan, 2015; Barbarey *et al*., 2024; Chen *et al*., 2020; Zawrah *et al*. 2022b). Various inorganic and organic fibres are used to reinforce geopolymer, including glass fibres, carbon, cotton, wool, cellulose, sweet sorghum, peat wood, sawdust, and wood (Paruthi *et al*., 2023). However, there has been limited research focused on reinforcement using inorganic oxides (Davidovits, 1991; Korniejenko *et al*., 2016; Lin *et al*., 2009; Lv *et al*., 2022; Matteo *et al*., 2021; Zawrah *et al*., 2020; Rashidi *et al*., 2024; Yan *et al*., 2016; Zawrah *et al*., 2021). Recently, one-dimensional MnO_2 (Feng *et al*., 2014; Ngida *et al*., 2020; Subramanian *et al*., 2005) nanostructures like nanowires/nanofibres/nanorods have generated great interest because of their excellent electrical, catalytic, optical, magnetic, and electrochemical properties (Feng *et al*., 2014; Li *et al*., 2005; Subramanian *et al*., 2005). This is due to their ease of preparation, low cost, and eco-friendly nature (Wang and Li, 2002). However, their applications as reinforcements in geopolymers remain limited. This work on geopolymer reinforced with MnO_2 nanofibre advances beyond prior studies on MnO_2 or other nanofibre reinforcements (e.g., TiO_2). This is because the study contributes to the growing body of knowledge by demonstrating the unique benefits of MnO_2 nanofibres in geopolymer systems (enhanced performance, cost effectiveness, sustainability, scalability, and broader applications), highlighting their potential for future advancements in material science. Different techniques have been applied to synthesis of MnO_2; those approaches include self-reacting microemulsion (Duan *et al*., 2012), co-precipitation (Li *et al*., 2006), solid-state reaction (Ngida *et al*., 2019), sono-chemical (Subramanian *et al*., 2005), and hydrothermal methods (Chin *et al*., 2010). The last technique is noteworthy for its ability to produce pure or multi-phase materials under mild conditions, such as controlled temperature and pH levels. However, in some cases, slight differences in morphology, size, phase composition, and crystallinity of synthesised materials might be altered when the reaction conditions are changed (Ding *et al*., 2006). Hydrothermal method has been easily utilised to prepare fine, stable/de-agglomerated, and homogeneous MnO_2 nanoparticles at low temperatures (Chin *et al*., 2002; Chin and Pang, 2010; Pang *et al*., 2000; Pang and Anderson, 2000; Xu *et al*., 2008). The objective of this study is to investigate the effect of chemically synthesised MnO_2 nanofibres on the physical and chemical properties of geopolymers fabricated from waste clay. The synthesised MnO_2 nanofibre is firstly characterised by different techniques, and then utilised as reinforcing agent for geopolymers. The prepared geopolymers are investigated for their phase composition, physical properties, and compressive strength by the suitable techniques. This means that the current study investigates the unexplored role of MnO_2 nanofibres in waste clay geopolymers, focusing on optimal dosage and mechanistic effects.

2. Materials and experimental procedures

2.1 Materials

In the present study, for hydrothermal synthesis of MnO_2, $KMnO_4$ (99%), manganese chloride tetrahydrate ($MnCl_2.4H_2O$) (99%), and NaOH pellets was utilised. All chemicals were purchased from Sigma-Aldrich and used as provided. On the other hand, for geopolymer fabrication, the feedstock waste clay, produced as a by-product from refractory production, was supplied by Asfour Company for Refractory in Egypt. Moreover, sodium silicate was supplied by Fisher Company, while NaOH pellets provided from Sigma-Aldrich were used in preparation of alkali activator.

2.2 Synthesis and investigation of MnO_2 nanofibres

It is well known that the hydrothermal method depends on reaction of aqueous mixtures that are heated above 100°C in a sealed reactor under generated pressure (Saoussen *et al*., 2015; Wu *et al*., 2006; Xu *et al*., 2008; Subramanian *et al*., 2008; Yan *et al*., 2009; Yuan *et al*., 2009; Zolfaghari *et al*., 2007). It has higher potential for preparation of material in industry without limitation than other methods. By controlling reaction conditions like time, temperature, pH and solvents, the desired properties of synthesised materials can be obtained easily in the lab and on industrial scales. For preparation of MnO_2 by hydrothermal method (Jeroen and Richard, 2005; Qiu *et al*., 2011; Teng, 2009; Wang and Li, 2002), typically 5.6 g $MnCl_2.4H_2O$ is dissolved in 100 ml de-ionised water, then $KMnO_4$ is added to the solution where the mass ratio between $KMnO_4$: $MnCl_2.4H_2O$ was 1:3. The prepared solution is stirred for 10 min, adjusting the pH value at 12–14 by alkaline solution. Subsequently, the obtained solution is moved into 100 ml Teflon-lined stainless steel autoclave and kept at 220°C for 48 h. After that, the autoclave is left to cool at ambient temperature and the obtained reaction product collected, filtered, washed by de-ionised water and acetone many times, then dried at 100°C for 24 h. The phase composition, morphology/particle size, and particle size distribution of synthesised MnO_2 nanofibres are investigated by X-ray diffraction (XRD) technique model Philips PW-1373, transmission electron microscope (TEM) type HRTEM JEOL JEM-2100 Japan operating at 120 kV and attached by selected area electron diffraction (SAED), as well as particle size analyser model Nano-ZS, Malvern instruments Ltd., UK, respectively. For testing the particle size distribution, the synthesised MnO_2 nanopowder is suspended in water and sonicated for 1 h before measuring at 25°C.

Downloaded from http://ftp.nowpublishers.com/jcoma/article-pdf/178/6/275/10176839/jcoma.25.00010en.pdf by guest on 05 August 2026

2.3 Fabrication and characterisation of geopolymers

Generally, the preparation of geopolymer pastes requires two essential components such as alkali activator and sources for alumino-silicates (Zawrah and Abo Sawan, 2023a, 2023b). The alkali activator was prepared by mixing of 12 M sodium hydroxide solution and sodium silicate solution with the ratio 1:3. The solution was prepared 24 h prior to the geopolymer preparation and kept away from atmosphere in order to maintain its stability and prevent its carbonation. The feeder's waste clay was firstly calcined at 850°C for 2 h to be converted into meta-kaolin (active source of alumino-silicate). The chemical analysis, as conducted by XRF technique, of calcined and uncalcined waste clays is given in Table 1. To prepare the reinforced geopolymer pastes, the alkali activator was well mixed with the calcined Feeder's clay and 0.1, or 0.3 or 0.5 wt.% of MnO_2 nanofibres, until getting workable and homogenous pastes. Table 2 illustrates the batch composition and NaO/SiO_2 ratio in alkali activator as well as SiO_2/Al_2O_3 ratio in the geopolymer. The reinforcement percentages were selected according to the previous studies dealing with the reinforcement by nanoparticles and also on the economic base (Abo Sawan *et al*., 2020; Zawrah *et al*., 2020, 2022b, 2025). To ensure homogeneity, the fibres were firstly mixed with alkali activator before adding the clay. Afterwards, the pastes were cast in acrylic moulds of dimensions 2.5 × 2.5 × 2.5 cm^3, and the moulds protected by a thin plastic cover to avoid evaporation of water. The covered moulds were kept in a lab oven for 24 h at 70°C (Abo Sawan *et al*., 2020; Zawrah *et al*., 2020, 2022a, 2025). The de-moulded samples were kept for 28 days in open air at room temperature, after which the samples were tested by different techniques. The dried specimens were subjected to various investigations such as chemical composition by XRD technique and infrared (FTIR model Jasco-300E Japan), physical properties (bulk density and apparent porosity) by the Archimedes principle, microstructure by scanning electron microscope (SEM) type QUANTA FEG250, and compressive strength by controlled hydraulic machine model SHIMADZU having maximum load 1000 kN and loading rate of 0.025 $kN/mm^2/s$.

3. Results and discussion

3.1 Phase composition, morphology and particle size distribution of synthesised MnO_2 nanofibres

One of the most important techniques used to identify the qualitative phase composition of materials is the XRD technique. Figure 1 shows the XRD pattern of synthesised MnO_2 nanofibres. The pattern indicates that the peaks are well defined for polycrystalline MnO_2 nanofibres, with no peaks from other phases, indicating their purity. The peaks are comparatively broad and short, confirming the semi-crystalline or amorphous nature and the nanoscale characteristics of the synthesised particles.

The TEM is usually utilized to investigate the morphology and size of the synthesised nanomaterials. Figure 2 shows TEM images with different magnifications (Figures 2(a) and 2(b)) and SAED pattern (Figure 2(c)) of hydrothermally synthesised MnO_2 nanofibres. It can be seen from Figure 2 that the synthesised MnO_2 consists of fibre-like nanoparticles with an average diameter less than 5 nm and an average length of about 100 nm. All particles have regular and homogeneous shape and size. All obtained nanofibres have smooth surfaces with consistent ends and straight sides. The synthesised MnO_2 nanofibres are polycrystalline with some agglomeration as indicated by SAED pattern that identifies the polycrystallinity of synthesised materials (Figure 2(c)). The driving force of MnO_2 nanofibre particle growth is attributed to the inherent crystal structure and its chemical potential. Through the hydrothermal process, spherical amorphous MnO_2 is firstly formed in the medium; after that the particles are grown and crystallised into nanofibres.

Table 1. Chemical analysis of uncalcined and calcined feeder's waste clay

Oxide	SiO_2	Al_2O_3	CaO	K_2O	TiO_2	MgO	SO_3	Fe_2O_3	L.O.I
Uncalcined	47.3	35.74	0.43	0.08	2.24	0.65	0.13	1.24	11.85
Calcined	56.04	37.92	0.53	0.1	3.01	0.7	0.17	1.38	0.21

Table 2. Batch composition of prepared geopolymers

Batch composition			Composition of alkali activator added: ml					
Waste clay: g	MnO_2 rod: g	Alkali activator: ml	Na_2O	SiO_2	H_2O	Na_2O/SiO_2 in alkali activator	Total SiO_2 in the batch: g	Total SiO_2/Al_2O_3
99.9	0.1	46	7.54	6.97	31.48	1.08	62.79	1.657
99.7	0.3	41	6.72	6.21	28.05	1.08	62.21	1.64
99.5	0.5	43.5	7.13	6.59	29.76	1.08	62.59	1.655

Downloaded from http://ftp.nowpublishers.com/jcoma/article-pdf/178/6/275/10176839/jcoma.25.00010en.pdf by guest on 05 August 2026

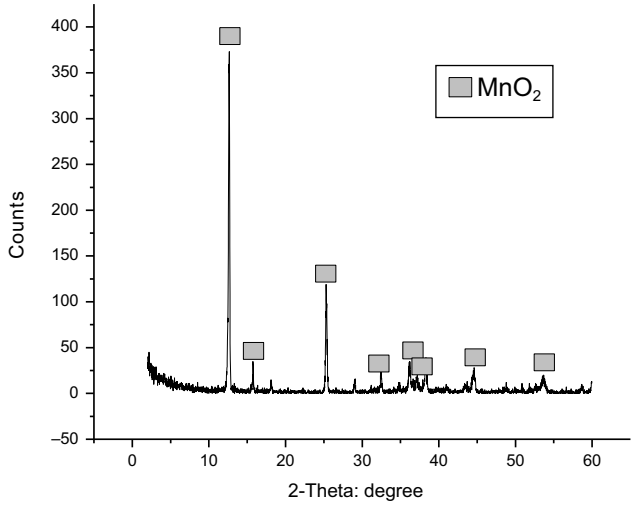

Figure 1. XRD pattern of synthesised MnO_2 nanofibres

Figure 3 shows the particle size distribution of prepared MnO_2 nanofibres. The figure indicates that two peaks with maximum intensities corresponding to particle sizes of 100 and 430 nm are observed; the intensities of these peaks represent approximately 6.4% and 93.6%, respectively. Generally, the particle size ranges between 25 and 800 nm with an average particle size of about 450 nm. Although the result of TEM indicated smaller size, larger sizes are obtained by particle size analyser due to agglomeration of the particles that might occur during preparation of the sample.

3.2 Properties of geopolymer reinforced with MnO_2 nanofibres

3.2.1 Mineralogical composition of geopolymers

Figure 4 depicts XRD patterns of geopolymers reinforced with different ratios of synthesised MnO_2 fibres. As indicated in the figure, the patterns of the prepared geopolymers are very similar to small deviations in peak intensity. It is widely recognised that geopolymers are semi-crystalline or amorphous materials primarily composed of sodium aluminum silicate hydrate or calcium aluminum silicate hydrate, depending on the alkalis or alkaline earth metals present in the starting materials. Figure 4 indicates the formation of semi-crystalline sodium aluminum silicate hydrate phase, in addition to the appearance of unreacted small amounts of quartz phase as indicated from its small peak intensity. According to the peak intensities of patterns detected for prepared geopolymers, it is noted that the sample that includes 0.3% MnO_2 nanofibres exhibits lower peak intensity related to sodium aluminum

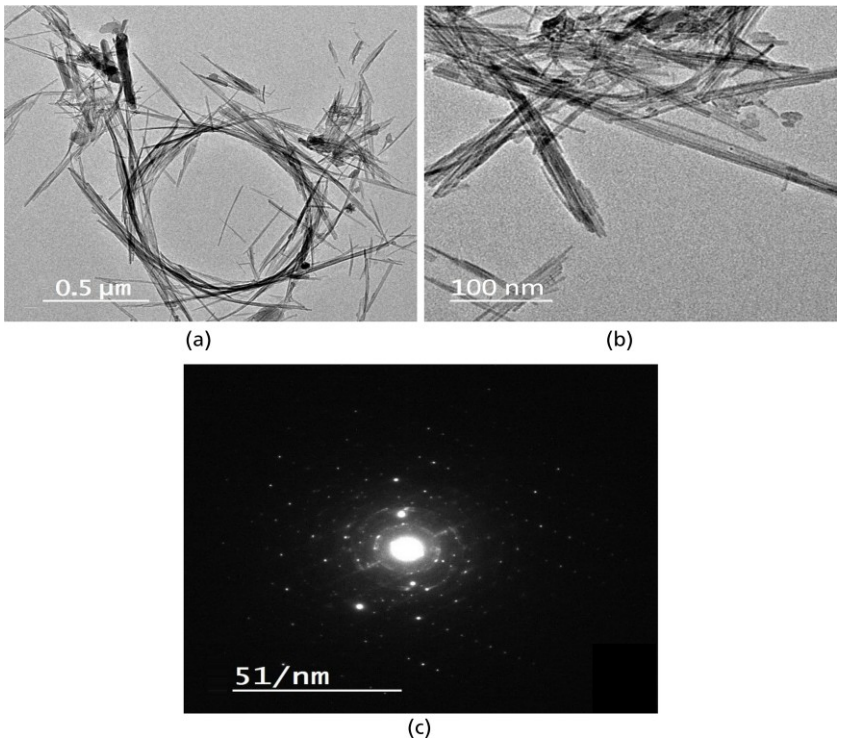

Figure 2. (a, b) TEM images and (c) SAED pattern of synthesised MnO_2 nanofibres

Downloaded from http://ftp.nowpublishers.com/jcoma/article-pdf/178/6/275/10176839/jcoma.25.00010en.pdf by guest on 05 August 2026

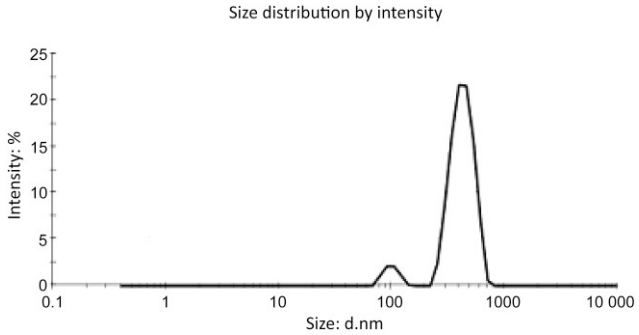

Figure 3. Particle size distribution of synthesised MnO_2 nanofibres

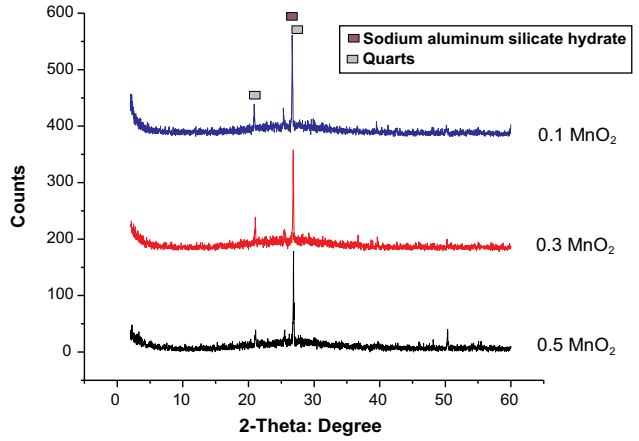

Figure 4. XRD patterns of prepared geopolymer samples that contain different ratios of MnO_2 nanorods

silicate hydrate phase indicating its higher polymerisation and amorphous nature. Chemically, it might be concluded that the optimum quantity of MnO_2 nanofibres needed to enhance the geopolymerisation process is 0.3%, after which the geopolymerisation might deteriorate due to the separation between the particles that might occur when the percentage of MnO_2 nanofibres is higher than 0.3%. When the added MnO_2 nanofibres are in the suitable range, they can display a dual effect; firstly, it can interact with the precursors, increases polymerisation, while secondly, it can act as reinforcement, interlocking the geopolymer matrix which consequently improves the mechanical properties.

The function groups in the formed geopolymer as detected by FTIR can confirm the composition identified by XRD (Abdel Aal *et al.*, 2014). Figure 5 represents the FTIR spectra of geopolymer reinforced with various percentages of MnO_2 nanofibres. FTIR can give a good insight on the effect of MnO_2 when

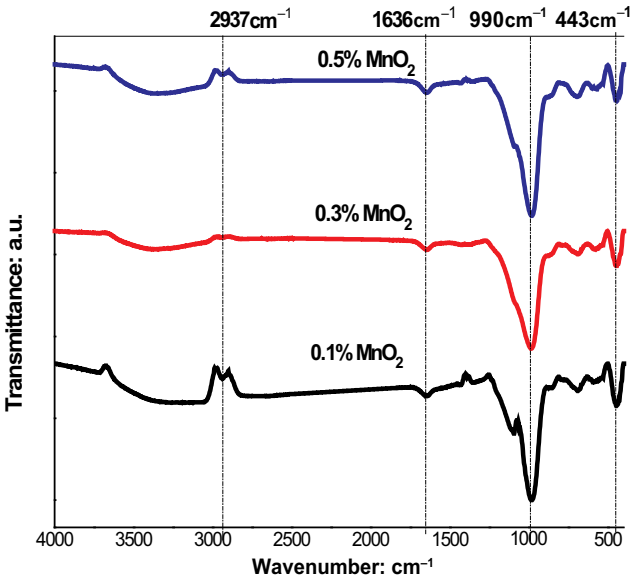

Figure 5. FTIR of geopolymers containing various ratios of MnO_2 nanofibres

imbedded inside the geopolymer structure, and can exhibit a new band in FTIR spectra. The broad band at 3200–3700 cm^{-1} and small band at 1639 cm^{-1} are related to the bending vibration and stretching of HOH and OH groups of water molecules produced from hydration of geopolymer. The main intense band centred at 990 cm^{-1}, within the range between 850 and 1250 cm^{-1} is attributed to asymmetric stretching vibration and flexural vibration of O–Al–O and Si–O–Al bands. The appearance of these bands indicates the formation of geopolymer networks. These bands show a slight shift in the wavenumber due to the incorporation of MnO_2 nanofibres, which alters the silicate network. The increased substitution of MnO_2 leads to polycondensation of Si–O–Mn bonds and changes in the chemical bonding within the system. The small band located at 1350–1400 cm^{-1} is assigned to asymmetric stretching of Si–O–Si bonds. This band is relatively high in geopolymers that include a lower amount of MnO_2, while with increasing MnO_2, the band vanishes, confirming the bonding of Mn with Si–O–Mn bonds. The characteristic bands at about 550 and 700 cm^{-1} indicate the amorphous nature of formed geopolymer or unreacted meta-kaolin. The short broad band in the range 443–500 cm^{-1} is assigned to O–Mn bonds.

It has been reported that the geopolymerisation process proceeded through condensation of alumino-silicate groups with alkali polysialate forming polymeric Al–O–Si bonds, that is, $M_n[-(Si–O_2)_z–Al–O]_n.wH_2O$, where M is the alkaline element, z is 1, 2, 3, and n is the degree of polycondensation (Abdel Aal *et al.*, 2014). Furthermore, the ideal composition of geopolymer should satisfy

Downloaded from http://ftp.nowpublishers.com/jcoma/article-pdf/178/6/275/10176839/jcoma.25.00010en.pdf by guest on 05 August 2026

the following oxide ranges: M_2O/SiO_2, 0.2–0.48; SiO_2/Al_2O_3, 3.3–4.5; H_2O/M_2O, 10–25; and M_2O/Al_2O_3, 0.8–1.6. The mechanism of geopolymerisation can be summarised by the following equations:

$$(Si_2O_5,\ Al_2O_2)n\ +\ 3nH_2O\ +\ NaOH\ or\ KOH\ \rightarrow n(OH)_3 - Si - O - \overset{(-)}{\underset{|}{Al}} - (OH)_3$$

$$n(OH)_3 - Si - O - \overset{(-)}{\underset{|}{Al}} - (OH)_3 + NaOH\ or\ KOH \rightarrow (Na, K) - \underset{|}{\overset{}{Si}} - \overset{(-)}{O} - \underset{|}{\overset{}{Al}} - O -)n + 3nH_2O$$

Orthosialate — (Na, K) − polysialate

$$(Si_2O_5, Al_2O_2)n\ +\ nSiO_2 + 4nH_2O\ +\ NaOH\ or\ KOH \rightarrow n(OH)_3 - Si - O - \overset{(-)}{\underset{(OH)_2}{Al}} - (OH)_3$$

$$n(OH)_3 - Si - O - \overset{(-)}{\underset{(OH)_2}{Al}} - (OH)_3 + NaOH\ or\ KOH \rightarrow (K, Na) - \left(\underset{|}{\overset{}{Si}} - O - \overset{(-)}{\underset{|}{Al}} - O - \underset{|}{\overset{}{Si}} - O - \right) n + 4nH_2O$$

Ortho (sialate − siloxo) — (Na, K) − polysailate − siloxo

3.2.2 Bulk density and apparent porosity of reinforced geopolymers

It is well known that physical properties such as apparent porosity and bulk density significantly impact and are widely used to assess material quality in various industries (Zawrah *et al*. 2018). The effect of MnO_2 nanofibre reinforcement content on the bulk density and apparent porosity is shown in Figure 6. It appeared that the apparent porosity reduces with increasing of MnO_2 ratio from 0.1% to 0.3%, and then increases again with increasing amount of MnO_2 up to 0.5%. This is attributed to increasing geopolymerisation after addition of 0.3% MnO_2 nanofibres followed by reduction of polymerisation after addition of higher amounts of MnO_2 nanofibres. Increasing geopolymerisation leads to reduction of open porosity while decreasing geopolymerisation leads to increasing open

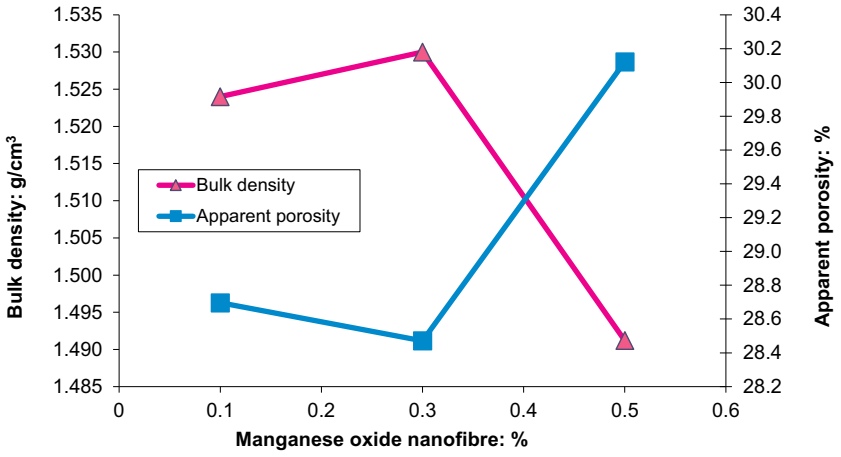

Figure 6. Bulk density and apparent porosity of geopolymers containing various ratios of MnO_2 nanofibres

Downloaded from http://ftp.nowpublishers.com/jcoma/article-pdf/178/6/275/10176839/jcoma.25.00010en.pdf by guest on 05 August 2026

porosity (Khale and Chaudhary, 2007). This means that the existence of a suitable amount of MnO_2 nanofibres (e.g., 0.3%) leads to enhancement of the geopolymerisation, while a higher amount of MnO_2 (e.g., 0.5%) reduces the geopolymerisation. Moreover, the differences in particle size between alumina, silica, and added MnO_2 nanofibres might play an important role in this phenomenon. The incorporation of a higher percentage of nanofibres (0.5%) deteriorates the geopolymerisation process and might prevent the connection of geopolymer networks which consequently increase the porosity. On the other side, bulk density goes in opposite trend to the apparent porosity, that is, it increases with decreasing porosity and vice versa.

3.2.3 Microstructure of reinforced geopolymers

Generally, SEM is applied to give good insight and information on the microstructural changes after the geopolymerisation process (Zawrah *et al*. 2018). The formed geopolymer gel networks in the matrix and their interconnection with the reinforcement are important features in the microstructure of reinforced geopolymer. The reinforcement of geopolymer by nanofibres is important in improving the mechanical properties and preventing the crack propagation. The direct boding, macro/micro/nanopores and their sizes, as well as pore size distribution are also interesting factors that have an effect on the physical and mechanical properties of geopolymers. Thus, it is important to examine the microstructure of fabricated geopolymers. Figure 7 shows SEM images (different magnifications) of geopolymers reinforced by various ratios of MnO_2 nanofibres, i.e., 0.1, 0.3, and 0.5 wt.%. It appears that all geopolymer samples exhibit gel structure with some unreacted starting materials and various degrees of porosity as well as voids. The first sample that includes 0.1% MnO_2 nanofibres includes agglomerated gel structure with large voids and some unreacted grains of metakaolin and quartz (as shown in Figures 7(a) and 7(b)). The reinforcing MnO_2 nanofibres are not detected between the gel matrices due to their small amounts in the sample. The fibres might interfere with the agglomerated geopolymer gel due to the magnetic properties of MnO_2. The radius of connected voids in this sample reaches about 50 μm. For the sample that contains 0.3% MnO_2 nanofibres (Figures 7(c) and 7(d)), the microstructure is relatively different. Condensed or fused-like gel structure without large voids is obtained. This microstructure includes some micro and nanopores. Very few fibre grains are also detected in this microstructure and most of fibres are embedded homogenously in the matrix. The gel structure appears as large lumps without aggregation into different small aggregates that form large voids. The gel structure is composed of nano-amorphous particles. When the percentage of MnO_2 nanofibres is increased to 0.5% (Figures 7(e) and 7(f)), agglomerated small lumps are formed, creating a large number of micro voids. This is probably due to the existence of higher amounts of MnO_2 nanofibres that act as separators for the gel structure. This increases the total porosity of this specimen as compared with the other two samples. The sizes of formed lumps range between 3 and 10 μm while the pore sizes between them range between 5 and 10 μm.

3.2.4 Compressive strength of reinforced geopolymers

The compressive strength of geopolymer materials reinforced by nanofibre is dependent on many factors such as the type and properties of fibres, the amount and volume of pores formed after geopolymerisation, the amount of formed geopolymer gel and the amount of unreacted phases (Zawrah *et al*., 2016). The relationship between compressive strength of prepared geopolymer and percentage of added MnO_2 nanofibres is shown in Figure 8. The compressive strength increases with the amount of added MnO_2 nanofibres up to 0.3 wt.%, then decreases again after addition of 0.5 wt.%. This is attributed to the formed compacted gel structure and lower porosity in the sample containing 0.3 wt.% MnO_2 nanofibres. In the sample containing 0.5 wt.% MnO_2, the increased number of voids and pores in the microstructure leads to a reduction in compressive strength. Moreover, it seems that 0.5 wt.% is not suitable and can make separation for geopolymer network structure which consequently enlarges the pores, volume and reduces the compressive strength. The compressive strength of the sample containing 0.5 wt.% MnO_2 nanofibres is lower than that of the sample containing 0.3 wt. but still relatively higher than that of the sample containing 0.1 wt.%. This is of course attributed to the variation of porosity and size of agglomerated lumps in all specimens. These results are confirmed by the data presented in Figure 9 which presents the relationship between compressive strength and apparent porosity. Opposite trends for compressive strength and apparent porosity are obtained in these results. In a previous study conducted by Zawrah *et al.* (2025), geopolymer reinforced by TiO_2 nanofibres was prepared. The study reported that the inclusion of TiO_2 nanofibres (0.3%) positively impacts the physical and mechanical properties, as well as the microstructure of the prepared geopolymers, by enhancing the geopolymerisation process, filling pores, and promoting interlocking within the microstructure. It is worth mentioning that the geopolymers are generally used for encapsulation of some materials and industrial wastes, thus, the geopolymer reinforced by MnO_2 nanofibres can exhibit a long-term stability without degradation over time.

4. Conclusions

(*a*) MnO_2 nanofibres were successfully synthesised by hydrothermal method using the suitable precursors. The diameter of the synthesised fibres was less than 5 nm and average length was of about 100 nm.

(*b*) Eco-friendly and cost-effective geopolymers with improved properties were successfully prepared from Feeder's waste clay and alkali activator. In addition, the properties of prepared geopolymer were enhanced by adding MnO_2 nanofibre as a reinforcing agent. On the industrial scale, the produced geopolymers can serve as alternatives to traditional cement-based materials that require significantly

Downloaded from http://ftp.nowpublishers.com/jcoma/article-pdf/178/6/275/10176839/jcoma.25.00010en.pdf by guest on 05 August 2026

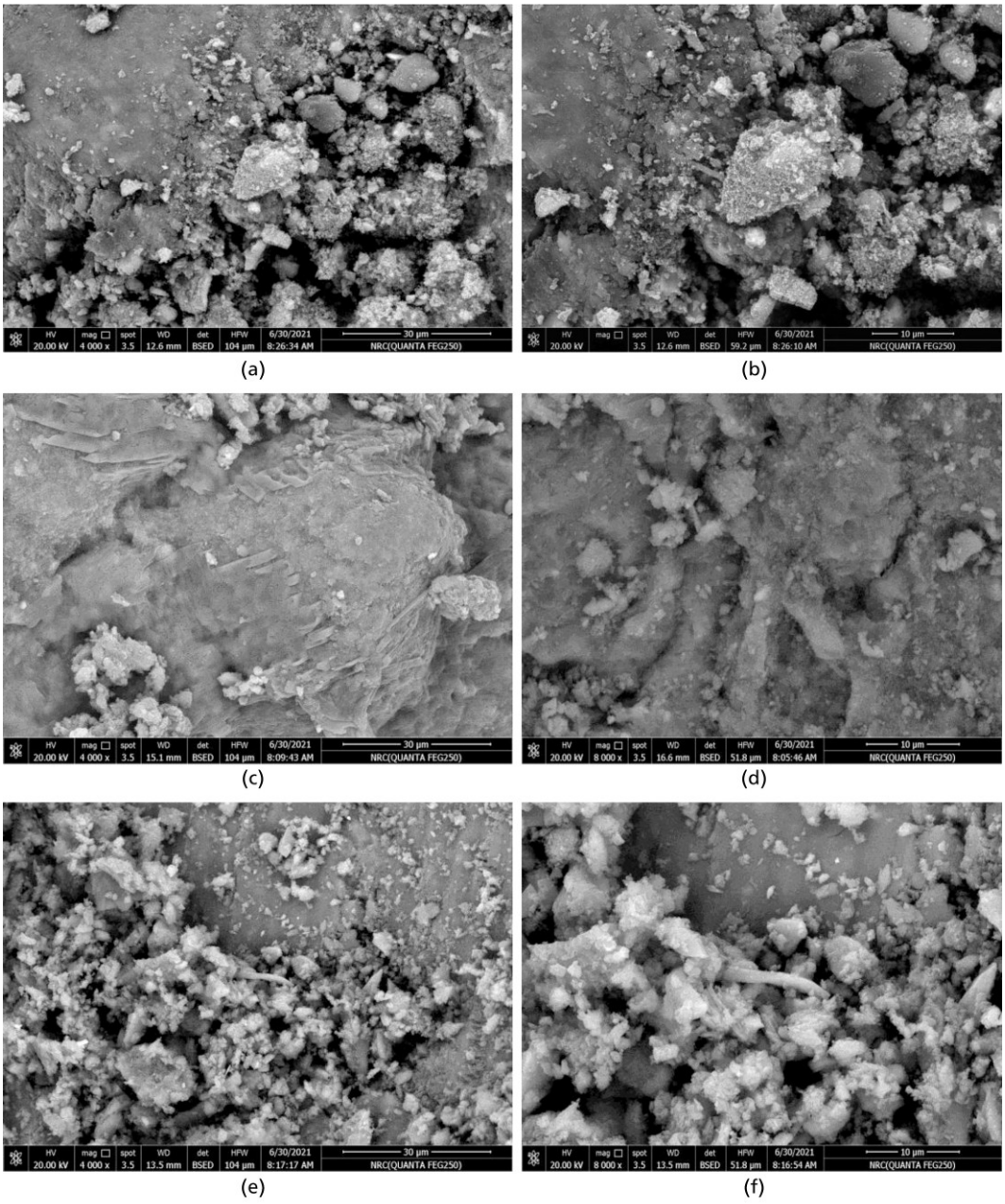

Figure 7. SEM images (different magnifications) of geopolymers containing various ratios of MnO_2 nanofibres

more energy for their production compared to geopolymers. The large quantities of waste clay available and the low cost of adding a small percentage of MnO_2 nanofibre make it easier to scale up this type of geopolymer.

(*c*) The physical properties, microstructure, and compressive strength of prepared geopolymers were improved after addition of 0.3 wt.% MnO_2 nanofibre, then deteriorated after addition of 0.5 wt.%. This higher percentage of MnO_2 nanofibre might cause gel structure separation with formation of highly porous microstructures that affect the compressive strength. The porosity decreased from 28.69% in the sample with 0.1 wt.% MnO_2 to 28.27% in the sample with 0.3 wt.% MnO_2. In addition, the strength increased from 23.43 to 27.97 MPa. This results in improvement percentages of 0.76% for porosity and 19.37% for strength, compared to the geopolymer sample containing 0.1% MnO_2.

Downloaded from http://ftp.nowpublishers.com/jcoma/article-pdf/178/6/275/10176839/jcoma.25.00010en.pdf by guest on 05 August 2026

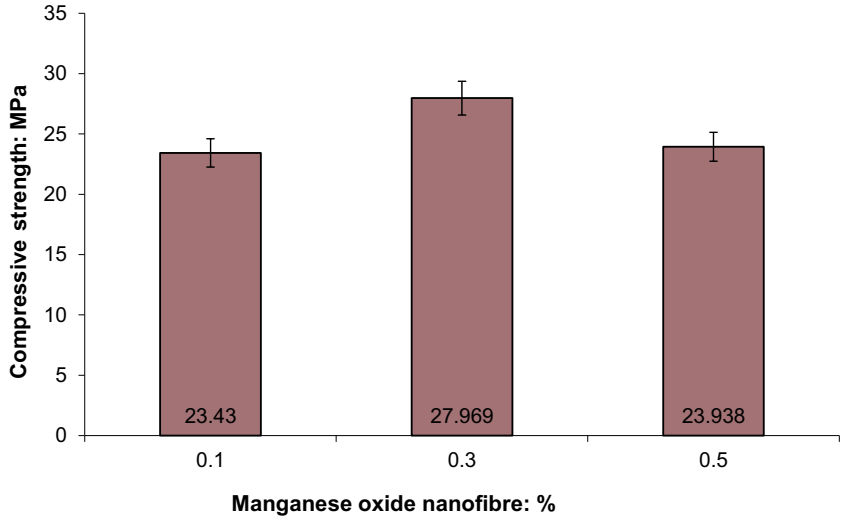

Figure 8. Compressive strength of geopolymers containing various ratios of MnO_2 nanofibres

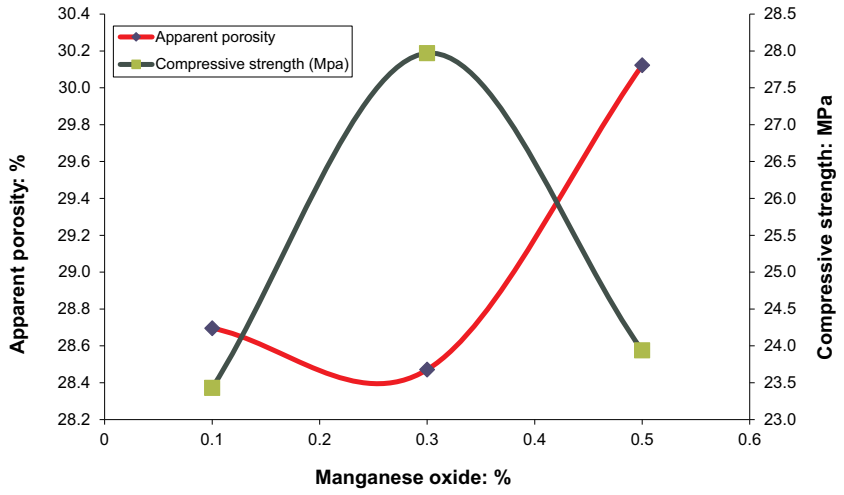

Figure 9. Apparent porosity versus compressive strength of geopolymers containing various ratios of MnO_2 nanofibres

(*d*) For the future directions, further studies such as thermal stability and durability are still recommended, taking into consideration the variation of raw and waste materials used for production of geopolymers.

Conflict of interest statement

The authors declare that they have no conflict of interest.

Author's contribution

M.F. suggested the plan of research and wrote the main manuscript text; S.E. and R.N. conducted the methodology; A.A. investigated the materials and supervised the research work. All authors reviewed the manuscript.

Funding

This work was funded by National Research Centre, Egypt, under Grant No. 12010417 (internal project).

REFERENCES

Abdel Aal A, Hammad TR, Zawrah MF, Battisha IK and Abou Hammad AB (2014) FTIR study of nanostructure perovskite $BaTiO_3$ doped with both Fe^{3+} and Ni^{2+} ions prepared by sol-gel technique. *Acta Physica Polonica A* **126(6)**: 1318–1321.

Abo Sawan SE, Zawrah MF, Khattab RM and Abdel-Shafi AA (2019) Fabrication, sinterabilty and characterization of non-colored and colored geopolymers with improved properties. *Material Research Express* **6(7)**.

Downloaded from http://ftp.nowpublishers.com/jcoma/article-pdf/178/6/275/10176839/jcoma.25.00010en.pdf by guest on 05 August 2026

Abo Sawan SE, Zawrah MF, Khattab RM and Abdel-Shafi AA (2020) In-situ formation of geopolymer foams through addition of silica fume: preparation and sinterability. *Materials Chemistry and Physics* **239**: 121998.

Arthiban K and Vaithianathan S (2015) Effect of kaolin content and alkaline concentration on the strength development of geopolymer concrete. *International Journal of ChemTech Research* **8(4)**: 1730–1734.

Barbarey MS, El-Sayed Seleman MM, El Kheshen AA and Zawrah MF (2024) Utilization of ladle furnace slag for fabrication of geopolymer: its application as catalyst for biodiesel production. *Construction and Building Materials* **411**: 134226.

Chen H, Zhang YJ, He PY, Li CJ and Liu LC (2020) Novel activated carbon route to low-cost geopolymer based porous composite with high mechanical resistance and enhanced CO_2 capacity. *Microporous and Mesoporous Materials* **305**: 110282.

Chin SF and Pang SC (2010) Tetrapropylammonium-manganese oxide/polypyrrole hybrid nanocomposite thin films as novel electrode materials for supercapacitors. *Materials Chemistry and Physics* **124(1)**: 29–32.

Chin SF, Pang SC and Anderson MA (2002) Material and electrochemical characterization of tetrapropylammonium manganese oxide thin films as novel electrode materials for electrochemical capacitors. *Journal of The Electrochemical Society* **149(4)**: A379–A384.

Chin SF, Pang SC and Anderson MA (2010) Self-assembled manganese dioxide nanowires as electrode materials for electro-chemical capacitors. *Materials Letters* **64(24)**: 2670–2672.

Davidovits J (1991) Inorganic polymeric new materials geopolymers. *Journal of Thermal Analysis* **37(8)**: 1633–1656.

Davidovits J (2020) *Geopolymer Chemistry and Applications*, 5th edn. Institut Géopolymère, Geopolymer Institute, Saint-Quentin, France.

Ding YS, Shen XF, Gomez S *et al.* (2006) Hydrothermal growth of manganese dioxide into three-dimensional hierarchical nanoarchitectures. *Advanced Functional Materials* **16(4)**: 549–555.

Duan X, Yang J, Gao H *et al.* (2012) Controllable hydrothermal synthesis of manganese dioxide nanostructures: shape evolution, growth mechanism and electrochemical properties. *CrystEngComm* **14(12)**: 4196–4204.

Feng L, Xuan Z, Zhao H *et al.* (2014) MnO_2 prepared by hydrothermal method and electro-chemical performance as anode for lithium-ion battery. *Nanoscale Research Letters* **9(1)**: 290–298.

Gailitis R, Sliseris J, Korniejenko K *et al.* (2020) Long-term deformation properties of a carbon fiber-reinforced alkali-activated cement composite. *Mechanics of Composite Materials* **56(1)**: 85–92.

Jeroen S and Richard IW (2005) Hydrothermal synthesis of the perovskite manganites $Pr_{0.5}Sr_{0.5}MnO_3$ and $Nd_{0.5}Sr_{0.5}MnO_3$ and alkali-earth manganese oxides $CaMn_2O_4$, 4H-$SrMnO_3$, and 2H-$BaMnO_3$. *Journal of Solid State Chemistry* **178**: 1683–1691.

Ke X and Baki VA (2021) Assessing the suitability of alkali-activated metakaolin geopolymer for thermochemical heat storage. *Microporous and Mesoporous Materials* **325**: 111329.

Khale D and Chaudhary R (2007) Mechanism of geopolymerization and factors influencing its development: a review. *Journal of Materials Science* **42(3)**: 729–746.

Korniejenko K, Frączek E, Pytlak E and Adamski M (2016) Mechanical properties of geopolymer composites reinforced with natural fibers. *Procedia Engineering* **151**: 388–393.

Korniejenko K, Łach M, Doğan Sağlamtimur N, Furtos G and Mikuła J (2020a) The overview of mechanical properties of short natural fiber reinforced geopolymer composites. *Environmental Research and Technology* **3(1)**: 28–39.

Korniejenko K, Lin W-T and Šimonová H (2020b) Mechanical properties of short polymer Fiber-Reinforced geopolymer composites. *Journal of Composites Science* **4(3)**: 128–122.

Łach M, Hebdowska-Krupa M, Mierzwi'nski D and Korniejenko K (2019) Mechanical properties of geopolymers reinforced with carbon and aramid long fibers. *IOP Conference Series: Materials Science and Engineering* **706(1)**: 012011.

Li Z, Ding Y, Xiong Y and Xie Y (2005) Rational growth of various γ-MnO_2 hierarchical structures and α-MnO_2 nanorods via a homo-geneous catalytic route. *Crystal Growth & Design* **5**: 1953–1958.

Li WN, Yuan J, Shen XF *et al.* (2006) Hydrothermal synthesis of structure- and shape-controlled manganese oxide octahedral molecular sieve nanomaterials. *Advanced Functional Materials* **16(9)**: 1247–1253.

Lin T, Jia D, Wang M, He P and Liang D (2009) Effects of fiber content on mechanical properties and fracture behavior of short carbon fiber reinforced geopolymer matrix composites. *Bulletin of Materials Science* **32(1)**: 77–81.

Lv C, Liu J, Guo G and Zhang Y (2022) The mechanical properties of plant fiber-reinforced geopolymers: a review. *Polymers* **14(19)**: 4134, 10.3390/polym14194134.

Matteo S, Abbas S and Marco V (2021) Recent advances in geopolymer technology. A potential eco-friendly solution in the construction materials industry: a review. *Journal of Composites Science* **5(109)**: 1–30.

Ngida REA, Zawrah MF, Khattab RM and Heikal E (2019) Hydrothermal synthesis, sintering and characterization of nano La-manganite perovskite doped with Ca or Sr. *Ceramics International* **45(4)**: 4894–4901.

Ngida REA, Zawrah MF, Khattab RM and Heikal E (2020) Utilization of leached MnO_2 for the mechanosynthesis of nano $La_xCa_{1-x}MnO_3$ and $LaxSr_{1-x}MnO_3$: Sinterability and properties. *Ceramics International* **46(3)**: 3433–3442.

Pang SC and Anderson MA (2000) Novel electrode materials for electrochemical capacitors: Part II. Material characterization of sol-gel-derived and electrodeposited manganese dioxide thin films. *Journal of Materials Research* **15(10)**: 2096–2106.

Pang SC, Anderson MA and Chapman TW (2000) Novel electrode materials for thin-film ultracapacitors: comparison of electrochemical properties of sol-gel-derived and electrodeposited manganese dioxide. *Journal of The Electrochemical Society* **147(2)**: 444–450.

Paruthi S, Rahman I, Husain A *et al.* (2023) A comprehensive review of nano materials in geopolymer concrete: Impact on properties and performance. *Developments in the Built Environment* **16**: 100287.

Qiu G, Huang H, Dharmarathna S *et al.* (2011) Hydrothermal synthesis of manganese oxide nano-materials and their catalytic and electrochemical properties. *Chemistry of Materials* **23(17)**: 3892–3901.

Rashidi S, Madani H, Maghsoudi M, Bameri M and Afzali M (2024) Multiscale assessment of microstructural features effects on mechanical and transport properties of ferro-silicomanganese/GGBFS-based alkali-activated composites. *Journal of Building Engineering* **88**: 109207.

Reckard W, Vickers L and Riessen A (2013) Performance of fiber reinforced, low density metakaolin geopolymers under simulated fire conditions. *Appl. Clay Sci* **73**: 71–77.

Samal S and Blanc I (2021) An application review of fiber-reinforced geopolymer composite. *Fibers* **9(4)**pp: 23–21.

Saoussen M, Mohamed B, Rafik M, Nassira CB and Mohamed O (2015) Critical behavior and the universal curve for magneto-caloric effect

Downloaded from http://ftp.nowpublishers.com/jcoma/article-pdf/178/6/275/10176839/jcoma.25.00010en.pdf by guest on 05 August 2026

in $Pr_{0.6}Ca_{0.1}Sr_{0.3}Mn_{1-x}Fe_xO_3$ (x = 0, 0.05 and 0.075) manganite. *J. Alloy. Compd* **633**: 207–215.

Silva FJ and Thaumaturgo C (2003) Fibre reinforcement and fracture response in geopolymeric mortars. *Fatigue & Fracture of Engineering Materials & Structures* **26**: 167–172.

Silva G, Kim S, Aguilar R and Nakamatsu J (2020) Natural fibers as reinforcement additives for geopolymers – a review of potential eco-friendly applications to the construction industry. *Sustainable Materials and Technologies* **23**: 132.

Subramanian S, Zhu H, Vajtai R, Ajayan PM and Wei B (2005) Hydrothermal synthesis and pseudocapacitance properties of MnO_2 nanostructures. *The Journal of Physical Chemistry. B* **109(43)**: 20207–20214.

Subramanian V, Zhu H and Wei B (2008) Alcohol-assisted room temperature synthesis of different nanostructured manganese oxides and their pseudocapacitance properties in neutral electrolyte. *Chemical Physics Letters* **453(4–6)**: 242–249.

Teng F (2009) Hydrothermal synthesis and their catalytic properties of manganite nanowires. *Solid State Sciences* **11(9)**: 1643–1648.

Wang X and Li Y (2002) Rational synthesis of α-MnO_2 single-crystal nanorods. *Chemical Communications (Cambridge, England)* (7): 764–765.

Wu J, Zhang H, Ma X *et al.* (2006) Synthesis and characterization of single crystalline MnOOH and MnO_2 nanorods by means of the hydrothermal process assisted with CTAB. *Materials Letters* **60(29–30)**: 3895–3898.

Xu C, Li B, Du H, Kang F and Zeng Y (2008) Electrochemical properties of nanosized hydrous manganese dioxide synthesized by a self-reacting microemulsion method. *Journal of Power Sources* **180(1)**: 664–670.

Yan D, Yan P, Cheng S *et al.* (2009) Fabrication, in-depth characterization and formation mechanism of crystalline porous birnessite MnO_2 film with amorphous bottom layers by hydrothermal method. *Crystal Growth & Design* **9(1)**: 218–222.

Yan B, Kasal L and Huang L (2016) A review of recent research on the use of cellulosic fibers, their fiber fabric reinforced cementitious, geo-polymer and polymer composites in civil engineering. *Composites Part B: Engineering* **92**: 94–132.

Yuan A, Wang X, Wang Y and Hu J (2009) Textural and capacitive characteristics of MnO_2 nanocrystals derived from a novel journal of nanomaterials solid-reaction route. *Electrochimica Acta* **54(3)**: 1021–1026.

Zawrah MF and Abo Sawan SE (2023a) Hardened and fired geopolymer mortars fabricated from cyclone's waste clay and submicron sand: a comparative study. *Construction and Building Materials* **364**: 129998.

Zawrah MF and Abo Sawan SE (2023b) Recycling of cyclones' waste clay for production of green and thermally stable geopolymers. *International Journal of Environmental Science and Technology* **20(11)**: 12719–12730.

Zawrah MF, Gado RA, Feltin N, Ducourtieux S and Devoille L (2016) Recycling and utilization assessment of waste fired clay bricks (grog) with granulated blast-furnace slag for geopolymer production. *Process Safety and Environmental Protection* **103**: 237–251.

Zawrah MF, Farag RS and Kohail MH (2018a) Improvement of physical and mechanical properties of geopolymer through addition of zircon. *Materials Chemistry and Physics* **217**: 90–97.

Zawrah MF, Gado RA and Khattab RM (2018b) Optimization of slag content and properties improvement of metakaolin-slag geopolymer mixes. *The Open Materials Science Journal* **12(1)**: 40–57.

Zawrah MF, Abo Sawan SE, Khattab RM and Abdel-Shafi AA (2020) Effect of nano sand on the properties of kaolin-based geopolymer: study on its low rate sintering. *Construction and Building Materials* **246**: 118486.

Zawrah MF, Badr HA, Khattab RM *et al.* (2021) Fabrication and characterization of non-foamed and foamed geopolymers from industrial waste clays. *Ceramics International* **47(20)**: 29320–29327.

Zawrah MF, Sadek HEH, Ngida REA, Abo Sawan SE and El-Kheshen AA (2022a) Effect of low-rate firing on physico-mechanical properties of unfoamed and foamed geopolymers prepared from waste clays. *Ceramics International* **48(8)**: 11330–11337.

Zawrah MF, Shehata N, Saddek AB and Ismail AG (2022b) Utilization of white-cement kiln dust in presence of raw/waste materials for production of alkali-activated products. *International Journal of Environmental Science and Technology* **19(9)**: 8573–8586.

Zawrah MF, Abo Sawan SE, Ngida REA and El-Kheshen AA (2025) Effect of TiO_2 nano fiber content on compressive strength of geopolymers fabricated from waste clay. *Journal of Material Engineering and Performance* **34**: 7693–7701

Zolfaghari A, Ataherian F, Ghaemi M and Gholami A (2007) Capacitive behavior of nanostructured MnO_2 prepared by sonochemistry method. *Electrochimica Acta* **52(8)**: 2806–2814.

How can you contribute?

To discuss this paper, please email up to 500 words to the editor at support@emerald.com. Your contribution will be forwarded to the author(s) for a reply and, if considered appropriate by the editorial board, it will be published as discussion in a future issue of the journal.

Proceedings journals rely entirely on contributions from the civil engineering profession (and allied disciplines). Information about how to submit your paper online is available at www.emeraldgrouppublishing.com/journal/jcoma, where you will also find detailed author guidelines.

Downloaded from http://ftp.nowpublishers.com/jcoma/article-pdf/178/6/275/10176839/jcoma.25.00010en.pdf by guest on 05 August 2026